Published OnlineFirst April 11, 2014; DOI: 10.1158/1078-0432.CCR-13-3169

Translational Relevance

In this study, we showed that the cell adhesion molecule 1 (CAMD1) versus CD7 plot reflects the progression of disease in patients infected with human T-cell lymphotrophic virus type I (HTLV-I), in that the proportion of $CADM1^{+}$ subpopulations (D, $CADM1^{pos}$ $CD7^{dim}$ and N, $CADM1^{pos}CD7^{neg}$) increased with the progression from HTLV-I asymptomatic carrier (AC) to indolent adult T-cell leukemia–lymphoma (ATL) to aggressive ATL. We confirmed the purity of the clonal HTLV-I–infected cells in these subpopulations of various clinical subtypes, including asymptomatic carriers. The results from the flow-cytometric analysis will help physicians assess disease status. The analysis is also practical in screening for putative high-risk HTLV-I asymptomatic carriers, which show nearly identical flow-cytometric and gene expression profiles with those of smoldering-type ATL patients. Furthermore, cell sorting by flow cytometry enables purification of clonally expanding cells in various stages of oncogenesis in the course of progression to aggressive ATL. Detailed molecular analysis of these cells will provide valuable information about the molecular events involved in multistep oncogenesis of ATL.

(indolent ATLs and HTLV-I asymptomatic carriers; AC) revealed that HTLV-I–infected and clonally expanded cells were purified similarly and that the subpopulations with downregulated CD7 grew concomitantly with the progression of HTLV-I infection (15). Although this type of flow-cytometric analysis was shown to be a useful tool, a substantial subpopulation of T cells shows downregulated expression of CD7 under physiologic (16, 17) and certain pathologic conditions, including autoimmune disorders, viral infection, and hematopoietic stem cell transplantation (18–23).

Recently, Sasaki and colleagues reported ectopic overexpression of the cell adhesion molecule 1/tumor suppressor in lung cancer 1 (CADM1/TSLC1) gene in primary acute-type ATL cells based on expression profile analysis (24, 25). CADM1 (/TSLC1) is a cell-adhesion molecule that was originally identified as a tumor suppressor in lung cancers (25, 26). In addition, numbers of $CD4^{+}$ $CADM1^{+}$ cells have been found to be significantly correlated with the proviral load (PVL) in both ATLs and HTLV-I asymptomatic carriers (25, 27). Thus, CADM1 is a good candidate marker of HTLV-I–infected cells. In the present study, we incorporated CADM1 into our flow-cytometric analysis. In the CADM1 versus CD7 plot of $CD4^{+}$ cells, HTLV-I–infected and clonally expanded cells were efficiently enriched in the $CADM1^{+}$ subpopulations regardless of disease status. In these cells, stepwise CD7 downregulation (from dimly positive to negative) occurred with disease progression. The proportion of the three subpopulations observed in this plot [P, $CADM1^{negative(neg)}CD7^{positive(pos)}$; D, $CADM1^{pos}CD7^{dim}$; and N, $CADM1^{pos}$ $CD7^{neg}$] accurately reflected the disease status in HTLV-I infection. The analysis of comprehensive gene expression in each subpopulation revealed that the expression profile of $CADM1^{+}$ subpopulations in indolent ATLs showed similarities with that in asymptomatic carriers with high PVL; yet, it was distinct from that in aggressive ATLs. These D and N subpopulations were indicative of HTLV-I–infected cells in the intermediate stage of ATL development.

Materials and Methods

Cell lines and patient samples

TL-Om1, an HTLV-I–infected cell line (28), was provided by Dr. Sugamura (Tohoku University, Sendai, Japan). The MT-2 cell line was a gift from Dr. Miyoshi (Kochi University, Kochi, Japan) and ST-1 was from Dr. Nagai (Nagasaki University, Nagasaki, Japan). Peripheral blood samples were collected from in-patients and out-patients at our hospital, as described in our previous reports (14, 15). As shown in Supplementary Table S1, 26 cases were analyzed (10 cases of asymptomatic carrier; 5 cases of smoldering-type; 6 cases of chronic-type; and 5 cases of acute-type). All patients with ATL were categorized into clinical subtypes according to Shimoyama's criteria (12, 29). Patients with various complications, such as autoimmune disorders and systemic infections, were excluded. Lymphoma-type patients were also excluded because ATL cells are not considered to exist in the peripheral blood of this clinical subtype. Samples collected from six healthy volunteers (mean age 48.8 years; range 34–66 years) were used as normal controls. The present study was approved by the Institutional Review Board of our institute (the University of Tokyo, Tokyo, Japan). Written informed consent was obtained from all patients and healthy volunteers.

Flow cytometry and cell sorting

Peripheral blood mononuclear cells (PBMC) were isolated from whole blood by density gradient centrifugation, as described previously (14). An unlabeled CADM1 antibody (clone 3E1) and an isotype control chicken immunoglobulin Y (IgY) antibody were purchased from MBL. These were biotinylated (primary amine biotinylation) using biotin N-hydroxysuccinimide ester (Sigma-Aldrich). Pacific Orange-conjugated anti-CD14 antibody was purchased from Caltag-Invitrogen. All other antibodies were obtained from BioLegend. Cells were stained using a combination of biotin-CADM1, allophycocyanin (APC)-CD7, APC-Cy7-CD3, Pacific Blue-CD4, and Pacific Orange-CD14. After washing, phycoerythrin-conjugated streptavidin was applied. Propidium iodide (Sigma-Aldrich) was added to the samples to stain dead cells immediately before flow cytometry. A FACSAria instrument (BD Immunocytometry Systems) was used for all multicolor flow cytometry and fluorescence-activated cell sorting (FACS). Data were analyzed using FlowJo software (TreeStar). The gating

Published OnlineFirst April 11, 2014; DOI: 10.1158/1078-0432.CCR-13-3169

procedure for a representative case is shown in Supplementary Fig. S1.

Quantification of HTLV-I proviral load by real-time quantitative PCR

PVL in FACS-sorted PBMCs was quantified by real-time quantitative PCR (TaqMan method) using the ABI Prism 7000 sequence detection system (Applied Biosystems), as described previously (14, 30).

Evaluation of HTLV-I *HBZ* gene amplification by semiquantitative PCR

HTLV-I *HBZ* gene amplification was performed as described previously (25). Briefly, the 25-μL PCR mixture consisted of 20 pmol of each primer, 2.0 μL of mixed deoxynucleotide triphosphates (2.5 mmol/L each), 2.5 μL of 10× PCR buffer, 1.5 μL of $MgCl_2$ (25 mmol/L), 0.1 μL of AmpliTaq Gold DNA Polymerase (Applied Biosystems), and 20 ng of DNA extracted from cell lines and clinical samples. The PCR consisted of initial denaturation at 94°C for 9 minutes, 30 cycles of 94°C for 30 seconds, 57°C for 30 seconds, and 72°C for 45 seconds, followed by 72°C for 5 minutes. The β-actin gene (*ACTB*) was used as an internal reference control. The primer sequences used were as follows: HBZ forward, 5′-CGCTGCCGATCACGATG-3′; HBZ reverse, 5′-GGAGGAATTGGTGGACG-3′; ACTB forward, 5′-CGTGCTCAGGGCTTCTT-3′; and ACTB reverse, 5′-TGAAGGTCTCAAACATGATCTG-3′. Amplification with these pairs of oligonucleotides yielded 177-bp HBZ and 731-bp β-actin fragments.

FISH for quantification of HTLV-I–infected cells

FISH analysis was performed to detect HTLV-I proviral DNA in mononuclear cells that had been FACS-sorted on the basis of the CADM1 versus CD7 plot. These samples were sent to a commercial laboratory (Chromosome Science Labo Inc.), where FISH analysis was performed. Briefly, pUC/HTLV-I plasmid containing the whole-HTLV-I genome was labeled with digoxigenin by the nick translation method, and was then used as a FISH probe. Pretreatment, hybridization, and washing were performed according to standard laboratory protocols. To remove fluorochrome-labeled antibodies attached to the cell surface, pretreatment consisted of treatment with 0.005% pepsin and 0.1 N HCl. The FISH probe was detected with Cy3-labeled anti-digoxigenin antibody. Cells were counterstained with 4′, 6 diamidino-2-phenylindole. The results were visualized using a DMRA2 conventional fluorescence microscope (Leica) and photographed using a Leica CW4000 cytogenetics workstation. Hybridization signals were evaluated in approximately 100 nuclei.

Inverse long PCR to assess the clonality of HTLV-I–infected cells

For clonality analysis, inverse long PCR was performed as described previously (14). First, 1 μg genomic DNA extracted from the FACS-sorted cells was digested with *PstI* or *Eco*RI at 37°C overnight. RNase A (Qiagen) was added to remove residual RNA completely. DNA fragments were purified using a QIAEX2 Gel Extraction Kit (Qiagen). The purified DNA was self-ligated with T4 DNA ligase (Takara Bio) at 16°C overnight. After ligation of the *Eco*RI-digested samples, the ligated DNA was further digested with *Mlu*I, which cuts the pX region of the HTLV-I genome and prevents amplification of the viral genome. Inverse long PCR was performed using Tks Gflex DNA Polymerase (Takara Bio). For the *Pst*I-treated group, the forward primer was 5′-CAGCCCATTCTATAGCACTCTCCAGGAGAG-3′ and the reverse primer was 5′-CAGTCTCCAAACACGTAGACTGGGTATCCG-3′. For the *Eco*RI-treated template, the forward primer was 5′-TGCCTGACCCTGCTTGCTCAACTCTACGTCTTTG-3′ and the reverse primer was 5′-AGTCTGGGCCCTGACCTTTTCAGACTTCTGTTTC-3′. Processed genomic DNA (50 ng) was used as a template. The reaction mixture was subjected to 35 cycles of denaturation (94°C, 30 seconds) and annealing plus extension (68°C, 8 minutes). Following PCR, the products were subjected to electrophoresis on 0.8% agarose gels. Fourteen patient samples were analyzed. For samples from which a sufficient amount of DNA was extracted, PCR was generally performed in duplicate.

Gene expression microarray analysis of each subpopulation in the CADM1 versus CD7 plot

Total RNA was extracted from each subpopulation in the CADM1 versus CD7 plot using TRIzol (Invitrogen) according to the manufacturer's protocol. Details of the clinical samples used for microarray analyses are shown in Supplementary Table S1. Treatment with DNase I (Takara Bio) was conducted to eliminate genomic DNA contamination. The quality of the extracted RNA was assessed using a BioAnalyzer 2000 system (Agilent Technologies). The RNA was then Cy3-labeled using a Low Input Quick Amp Labeling Kit (Agilent Technologies). Labeled cRNA samples were hybridized to 44K Whole Human Genome Oligonucleotide Microarrays (Agilent Technologies) at 65°C for 17 hours. After hybridization, the microarrays were washed and scanned with a Scanner C (Agilent Technologies). Signal intensities were evaluated by Feature Extraction 10.7 software and then analyzed using Gene Spring 12.0 software (Agilent Technologies). Unsupervised two-dimensional hierarchical clustering analysis (Pearson correlation) was performed on 10,278 genes selected by one-way ANOVA ($P < 0.05$). The dataset for these DNA microarrays has been deposited in Gene Expression Omnibus (accession number GSE55851).

Expression analysis of miR-31 and *Helios* transcript variants of each subpopulation in the CADM1 versus CD7 plot

The expression levels of the microRNA miR-31 were quantified using a TaqMan-based MicroRNA Assay (Applied Biosystems), as described previously (31), and normalized to RNU48 expression level. Helios mRNA transcript variants were examined using reverse transcription

Published OnlineFirst April 11, 2014; DOI: 10.1158/1078-0432.CCR-13-3169

PCR (RT-PCR) with Platinum Taq DNA Polymerase High Fidelity (Invitrogen), as described previously (32). To detect and distinguish alternative splicing variants, PCR analyses were performed with sense and antisense primer sets specific for the first and final exons of the Helios gene. The PCR products were then sequenced to determine the exact type of transcript variant. A mixture of Hel-1, Hel-2, Hel-5, and Hel-6 cDNA fragments was used as a "Helios standard" in the electrophoresis of RT-PCR samples.

Results

CADM1 expression based on the CD3 versus CD7 plot in CD4$^+$ cells in primary HTLV-I–infected blood samples

The clinical profiles of the 32 cases analyzed are shown in Supplementary Table S1. We first examined CADM1 expression in each subpopulation (H, I, and L) of the CD3 versus CD7 plot. Representative data (for a case of smoldering ATL) are shown in Fig. 1A. The results demonstrate that

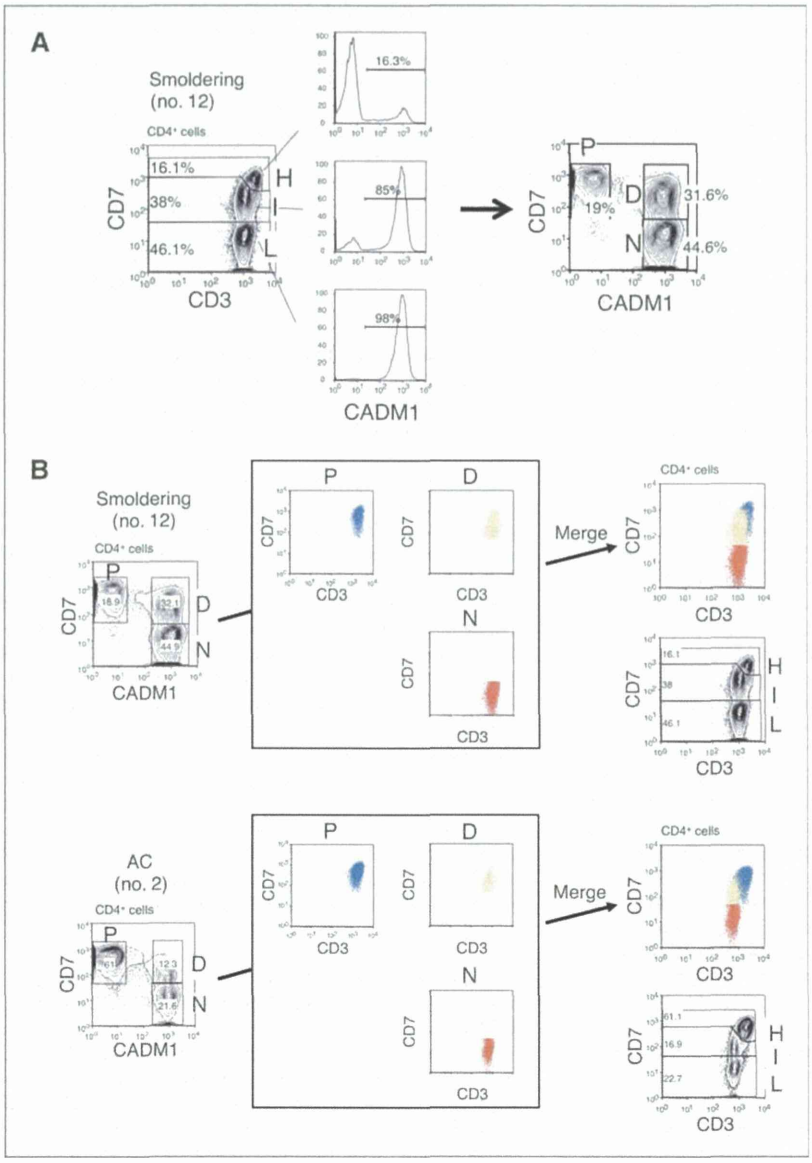

Figure 1. CADM1 versus CD7 plot for CD4$^+$ cells from HTLV-I–infected blood samples analyzed by flow cytometry. A, representative flow-cytometric analysis of a patient with smoldering-type ATL. Three subpopulations (H, I, and L) were observed in the CD3 versus CD7 plot for CD4$^+$ cells (left). Expression of CADM1 in each subpopulation is shown (middle). The right-hand panel shows how the CADM1 versus CD7 plot for CD4$^+$ cells was constructed. B, the P, D, and N subpopulations in the CADM1 versus CD7 plot correspond to the H, I, and L subpopulations in the CD3 versus CD7 plot. Blue, yellow, and red dots, respectively, indicate the P, D, and N subpopulations in the CADM1 versus CD7 plot, and are redrawn in the CD3 versus CD7 plot. Two representative cases are shown. In the upper case, the P and D subpopulations in the CADM1 versus CD7 plot are partly intermingled in the CD3 versus CD7 plot. Unlike the CD3 versus CD7 plot, the CADM1 versus CD7 plot clearly distinguishes three subpopulations.

Published OnlineFirst April 11, 2014; DOI: 10.1158/1078-0432.CCR-13-3169

CADM1 was expressed almost exclusively in the I and L subpopulations. Drawing a CADM1 versus CD7 plot for $CD4^+$ cells revealed three distinct subpopulations (P, $CADM1^{neg}CD7^{pos}$; D, $CADM1^{pos}CD7^{dim}$; and N, $CADM1^{pos}$ $CD7^{neg}$). As shown in Fig. 1B, the P, D, and N subpopulations corresponded to the H, I, and L subpopulations in the CD3 versus CD7 plot. In the previous CD3 versus CD7 plot, the lower case (AC no. 2) showed three distinct subpopulations. However, in the upper case (smoldering no. 12), the H and I subpopulations substantially intermingled with each other and were not clearly separated. In contrast, the CADM1 versus CD7 plot clearly revealed three distinct subpopulations in both cases.

HTLV-I–infected cells are highly enriched in $CADM1^+$ subpopulations

On the basis of previous reports (25, 27), we expected HTLV-I–infected cells to be enriched in the $CADM1^+$ subpopulations in our analysis. Figure 2A shows the PVL measurements of the three subpopulations in the CADM1 versus CD7 plot for three representative cases. HTLV-I–infected cells were highly enriched in the $CADM1^+$ subpopulations (D and N). The PVL data indicate that most of the cells in the D and N subpopulations were HTLV-I infected. Figure 2B shows the results of semiquantitative PCR of the *HBZ* gene in representative cases. In the D and N subpopulations, the *HBZ* gene was amplified to the same degree as in the HTLV-I–positive cell line. To confirm these results, FISH was performed in one asymptomatic carrier. As shown in Supplementary Fig. S2, HTLV-I–infected cells were highly enriched in the D and N subpopulations, which supports the results of the PVL analysis and semiquantitative PCR of the *HBZ* gene. In the FISH analysis, percentages of HTLV-I–infected cells in D and N did not reach 100%. This may have been due to a technical issue. Because the cells subjected to FISH analysis were sorted by FACS, several fluorochrome-conjugated antibodies may have remained on their surfaces, even after treatment with protease.

The CADM1 versus CD7 plot accurately reflects disease progression in HTLV-I infection

Compared with the CD3 versus CD7 plot, the CADM1 versus CD7 plot was revealed to be clear in its distinction of the three subpopulations and efficient in enrichment of HTLV-I–infected cells. On the basis of these findings, we analyzed clinical samples of asymptomatic carriers and three clinical subtypes of ATL: the smoldering, chronic, and acute subtypes. Data for representative cases, presented in Fig. 3A, suggest that the continual changes in the proportions of the three subpopulations are associated with disease progression. In the CADM1 versus CD7 plot, normal control samples showed a P-dominant pattern. With progression of the disease from the asymptomatic carrier state with a low PVL to that with a high PVL, and to indolent-type ATL, the D and N subpopulations increased gradually. As the disease further progressed to acute-type ATL, the N subpopulation showed remarkable expansion. Data for all analyzed samples are presented in Fig. 3B. The results suggest that the CADM1 versus CD7 plot of peripheral blood samples represents progression of the disease in HTLV-I carriers. Data for the normal control cases analyzed are shown in Supplementary Fig. S3. In all normal controls, the percentages of the D and N subpopulations were low. Supplementary Fig. S4 shows temporal data for a patient with chronic-type ATL who progressed from stable disease to a relatively progressive state and the concomitant change in the flow cytometry profile.

Clonality analysis of the three subpopulations in the CADM1 versus CD7 plot

To characterize the three subpopulations further, the clonal composition of each subpopulation was analyzed by inverse long PCR, which amplifies part of the provirus

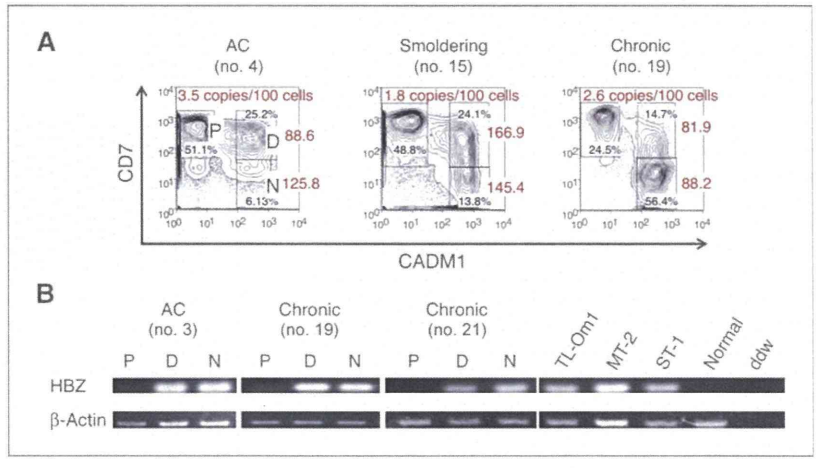

Figure 2. HTLV-I–infected cells are highly enriched in the $CADM1^+$ subpopulations. A, analysis of PVL in the three subpopulations. Three representative cases are shown. PVL data (copies/100 cells) are shown in red. Percentages of each subpopulation are shown in black. B, semiquantitative PCR of the *HBZ* gene in the three subpopulations in three representative cases. Normal, DNA from PBMCs from a normal control; ddw, deionized distilled water.

Published OnlineFirst April 11, 2014; DOI: 10.1158/1078-0432.CCR-13-3169

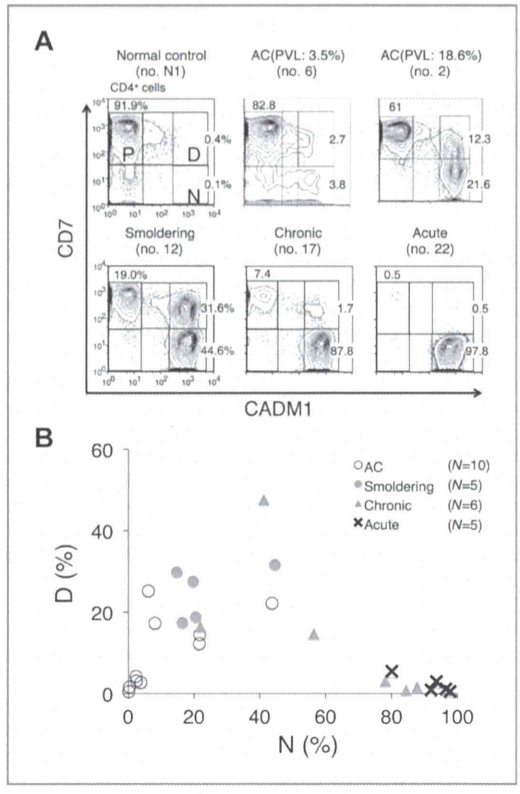

Figure 3. Proportion of each subpopulation in the CADM1 versus CD7 plots for asymptomatic HTLV-I carriers (asymptomatic carriers) and ATLs of various clinical subtypes. A, data of representative cases are shown. B, a two-dimensional plot of all analyzed samples showing the percentages of the D and N subpopulations.

long terminal repeat and the flanking genomic sequence of the integration sites. Cells in each subpopulation were sorted by FACS, and subjected to inverse long PCR analysis. Representative results for smoldering-, chronic-, and acute-type ATL samples are presented in Fig. 4A. Major clones, indicated by intense bands, were detected in the D and N subpopulations. The major clones in the D and N subpopulations in each case were considered to be the same based on the sizes of the amplified bands, suggesting that clonal evolution is accompanied by downregulation of CD7 expression. Fig. 4B shows representative results for three cases of asymptomatic carrier. In all cases, weak bands in the P subpopulation were visible, indicating that this population contains only minor clones. In these asymptomatic carriers, the proportion of abnormal lymphocytes and PVL increases from left to right. The consistent increase in the D and N subpopulations, together with growth of major clones as shown in the inverse PCR analysis, were considered to reflect these clinical data.

Gene expression profiling of the three subpopulations in the CADM1 versus CD7 plot

To determine the molecular basis for the biologic differences among the three subpopulations in the CADM1 versus CD7 plot, we next characterized the gene-expression profiles of the subpopulations of the following clinical subgroups: asymptomatic carriers ($n = 2$), smoldering-type ATLs ($n = 2$), chronic-type ATL ($n = 1$), acute-type ATLs ($n = 3$), and normal controls ($n = 3$). The two asymptomatic carriers (nos. 5 and 9) had high PVLs (11.6 and 26.2%, respectively) and relatively high proportions of D and N subpopulations (Supplementary Table S1). Unsupervised hierarchical clustering analysis of the results revealed three clusters (A, B1, and B2) or two major clusters A and B, where A is composed solely of the samples of the acute-type N subpopulation and B is subdivided into two clusters (B1 and B2; Fig. 5A). The B2 cluster is composed of the P subpopulation of all clinical subtypes and of normal controls, whereas the B1 cluster is composed of the D and N subpopulations of

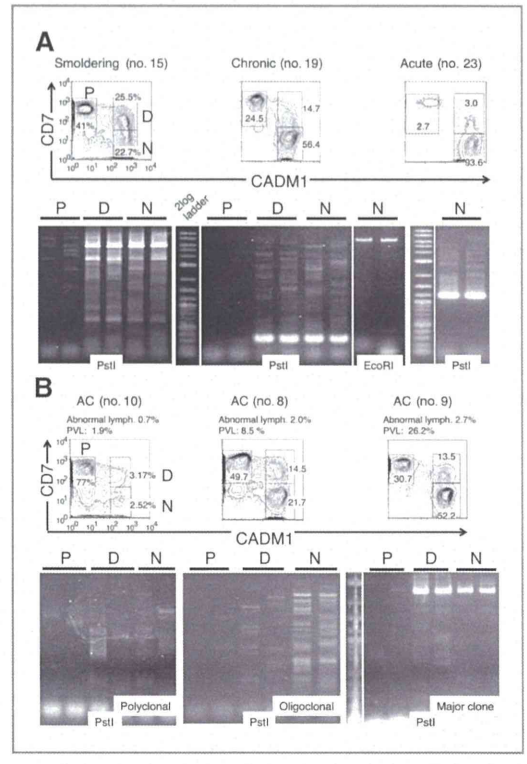

Figure 4. Clonality of subpopulations in the CADM1 versus CD7 plot analyzed by inverse long PCR. FACS-sorted cells (P, D, and N) were subjected to inverse long PCR. The black bar indicates duplicate data. Flow-cytometric profiles and clinical data are also presented. A, representative cases of smoldering-, chronic-, and acute-type ATL are shown. B, representative cases of asymptomatic carriers are shown.

Published OnlineFirst April 11, 2014; DOI: 10.1158/1078-0432.CCR-13-3169

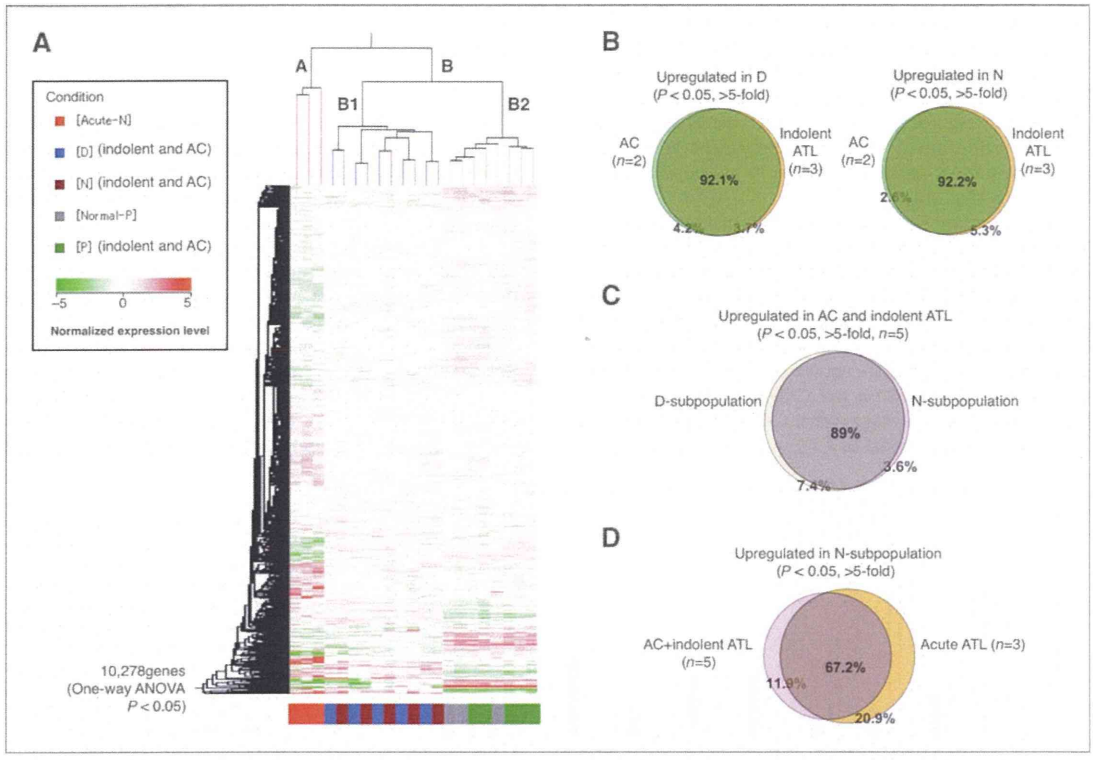

Figure 5. Comprehensive gene expression analysis of the three subpopulations in the CADM1 versus CD7 plot. A, we conducted an unsupervised hierarchical clustering analysis of 10,278 genes whose expression levels were significantly changed in the P subpopulation of normal controls ($n = 3$); P, D, and N subpopulations of asymptomatic carriers and indolent ATLs ($n = 5$); and N subpopulation of acute-ATLs ($n = 3$; one-way ANOVA, $P < 0.05$). The P and D subpopulations of acute ATLs and D and N subpopulations of normal controls could not be analyzed because of insufficient numbers of cells. Clustering resulted in three major clusters: (i) P subpopulations of normal controls (gray) and asymptomatic carriers/indolent ATLs (green); (ii) D and N subpopulations of asymptomatic carriers/indolent ATLs (blue and brown, respectively); and (iii) N subpopulations of acute ATLs (red). These results indicate that the P subpopulations of asymptomatic carriers/indolent ATLs have characteristics similar to those of normal uninfected cells, whereas the D and N subpopulations of asymptomatic carriers/indolent ATLs have genetic lesions in common. The N subpopulations of acute ATLs are grouped in an independent cluster, meaning that these malignant cell populations have a significantly different gene expression profile, even compared with the N subpopulations of indolent ATLs. B, similarity between asymptomatic carriers and indolent ATLs. The Venn diagrams show that 92.1% and 92.2% of genes upregulated in the D and N subpopulations, respectively, compared with "Normal-P" ($P < 0.05$), were common to asymptomatic carriers ($n = 2$) and indolent ATLs ($n = 3$). C, similarity between the D and N subpopulations. The Venn diagram shows that 89% of genes upregulated in the D and N subpopulation, compared with Normal-P ($P < 0.05$), overlapped. D, comparison of the N subgroups between acute-ATLs ($n = 3$) and asymptomatic carriers/indolent ATLs ($n = 5$). As shown in the Venn diagram, 67.2% of genes were upregulated ($P < 0.05$) in the N subpopulations of both acute ATLs and asymptomatic carrier/indolent ATLs. However, a significant number of genes (20.9%) were upregulated only in the N subpopulation of acute ATLs.

asymptomatic carriers and indolent ATLs (smoldering- and chronic-type).

Figure 5B shows a Venn diagram of the upregulated genes in the D subpopulation (left) or the N subpopulation (right) common to asymptomatic carriers ($n = 2$) and indolent ATLs ($n = 3$). These diagrams demonstrate that the changes in the gene expression profiles of the D and N subpopulations of asymptomatic carriers were similar to those of indolent ATLs. Furthermore, the gene expression profiles of the D and N subpopulations of asymptomatic carriers and indolent ATLs were similar (Fig. 5C). In contrast, the upregulated genes showed distinct differences between the N subpopulation of acute-type ATL and that of indolent ATLs and asymptomatic carriers, although approximately 70% were common to both (Fig. 5D).

Expression of a tumor suppressor microRNA and splicing abnormalities of Ikaros family genes in the three subpopulations

To determine whether the novel subpopulations identified had other properties in common with ATL cells, we examined miR-31 levels and *Helios* mRNA patterns in sorted subpopulations (31, 32). Expression of miR-31 decreased drastically in the D subpopulation derived from indolent ATLs and asymptomatic carriers, and was

Published OnlineFirst April 11, 2014; DOI: 10.1158/1078-0432.CCR-13-3169

even lower in the N subpopulation derived from asymptomatic carriers and indolent/acute ATLs (Fig. 6A). In addition, examination of *Helios* mRNA transcript variants revealed that expression levels of *Hel-2*, which lacks part of exon 3, were upregulated in the D and N subpopulations of asymptomatic carriers and indolent ATLs, and it was dominantly expressed in the N subpopulation of acute ATLs (Fig. 6B).

Supplementary Fig. S5 presents a summary of this study. The representative flow-cytometric profile shows how the CADM1 versus CD7 plot reflects disease progression in HTLV-I infection. The plot together with the gene expression profiles clearly distinguished the subpopulations of distinct oncogenic stages. The groups classified according to gene expression profile are shown as blue, yellow, and red and are superimposed on the CADM1 versus CD7 plot. Collectively, our data suggest that CADM1 expression and stepwise downregulation of CD7 were closely associated with clonal expansion of HTLV-I–infected cells in ATL progression.

Discussion

We showed that the CADM1 versus CD7 plot is capable of discriminating clonally expanding HTLV-I–infected cells in indolent ATLs and even in asymptomatic carriers, as well as in acute-type ATLs. Our analysis demonstrated efficient enrichment of HTLV-I–infected cells in the $CADM^+$ subpopulations (D and N in the CADM1 vs. CD7 plot), based on the results of real-time PCR (PVL analysis), semiquantitative PCR analysis of the *HBZ* gene, and FISH analysis (Fig. 2 and Supplementary Fig. S2). Furthermore, the CADM1 versus CD7 plot was shown to discriminate the three subpopulations more clearly than the CD3 versus CD7 plot (Fig. 1). Clonality analysis of ATLs and asymptomatic carriers (Fig. 4A and B) revealed that $CADM1^+$ subpopulations (D and N) contained

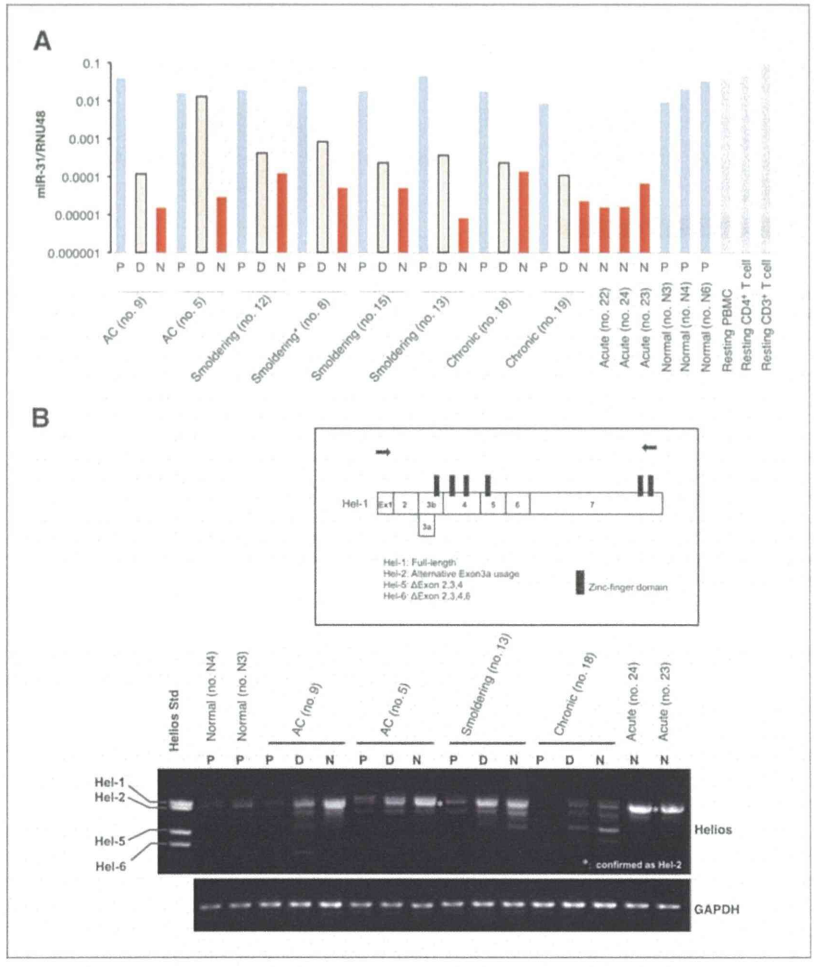

Figure 6. Gene expression pattern in the CADM1/CD7 subpopulation. A, miR-31 expression levels quantified by TaqMan-based real-time PCR. Total RNAs derived from each subpopulation were isolated and analyzed by RT-real-time PCR. RNU48 levels were also measured as an internal normalizer. *Smoldering (no. 8), this patient was considered to be at the asymptomatic carrier/smoldering borderline, because the proportion of abnormal lymphocytes fluctuated around 5%. On the day of sampling, the patient's hemogram showed 6.5% abnormal lymphocytes. B, expression analysis of *Helios* transcript variants in the subpopulations of normal controls ($n = 2$), asymptomatic carriers ($n = 2$), and ATLs (smoldering-type ATL, $n = 1$; chronic-type ATL, $n = 1$; acute-type ATL, $n = 2$). Comparisons of transcript variants among the P, D, and N subpopulations were performed by RT-PCR using primer sets specific for full-length *Helios* cDNA (top). The primer locations for *Helios* PCR are indicated by arrows in the schematic representation of *Hel-1*. The amplified cDNA (asterisk) was confirmed to be the *Hel-2* variant. The *Helios* standard (left lane), a mixture of cDNA fragments of *Hel-1*, *Hel-2*, *Hel-5*, and *Hel-6*, was used as a size indicator for each transcript variant. The glyceraldehyde-3-phosphate dehydrogenase (*gapdh*) mRNA was analyzed as an internal control (bottom).

Published OnlineFirst April 11, 2014; DOI: 10.1158/1078-0432.CCR-13-3169

clonally expanded HTLV-I–infected cells, whereas cells in the P subpopulation ($CADM1^-$) did not show clonal expansion in this analysis. Current molecular analyses of ATL cells have been limited to HTLV-I–infected cell lines and primary cells from acute/lymphoma type ATL, because in these cases, the predominant expanding clones are readily available with relatively high purity. However, the separation of clonally expanding ATL cells from indolent ATLs and asymptomatic carriers has not yet been achieved. The CADM1 versus CD7 plot from FACS allows efficient purification of such clones *in vitro*.

In an unsupervised clustering analysis of the gene expression data, the D and N subpopulations of asymptomatic carriers/indolent ATLs were grouped together, suggesting that the biologic characteristics of these subpopulations are similar (Fig. 5A and B) but distinct from the N subpopulation of acute-type ATLs (Fig. 5D). These results support the notion that in indolent ATLs and even in asymptomatic carriers, the D and N subpopulations are clonally expanding cells representing the intermediate oncogenic stage. Although the D and N subpopulations have similar gene expression profiles (Fig. 5C), there are potentially important differences distinguishing these subpopulations, according to the apparent decrease in the D subpopulation and increase in the N subpopulation that were observed as the disease progressed from indolent to acute-type ATL (Fig. 3). Detailed analysis of the genomic and epigenomic differences between these two subpopulations will provide us with information about the genomic and epigenomic lesions that are involved in disease progression. Another important finding is that the expression profiles of cells in the N subpopulation of indolent and acute-type ATLs showed significant differences, even though the majority of the genes were common to both groups (Fig. 5D). Characterization of the genes that show distinct expression patterns will reveal the molecular events that contribute to the progression from indolent to aggressive ATLs.

To address whether the emerging molecular hallmark of ATL was conserved in the novel subpopulations identified, we examined the miR-31 level and *Helios* mRNA pattern in sorted subpopulations (Fig. 6). Through integrative analyses of ATL cells, we recently showed that the expression of miR-31, which negatively regulates noncanonical NF-κB signaling by targeting NIK, is genetically and epigenetically suppressed in ATL cells, leading to persistent NF-κB activation, and is thus inversely correlated with the malignancy of the cells (31). The miR-31 levels in the P subpopulations in asymptomatic carriers and indolent ATLs were as high as those in normal P subpopulations, PBMCs, and resting T cells, whereas those in the D subpopulations decreased significantly and those in the N subpopulations were as low as in acute-type N subpopulations (Fig. 6A). Previously, we also identified ATL-specific aberrant splicing of *Helios* mRNA and demonstrated its functional involvement in ATL (32). As shown in Fig. 6B, the *Hel-2* type variant, which lacks part of exon 3 and thus lacks one of the four DNA-binding zinc-finger domains, accumulated in the D and N subpopulations of asymptomatic carriers and indolent ATLs, and was dominantly expressed in the N subpopulation of acute-type ATLs. Collectively, the molecular abnormality of ATL cells became evident in the gradual progression from P to D to N, even in asymptomatic carriers, strongly supporting the notion that the CADM1/CD7 expression pattern correlates with the multistep oncogenesis of ATL.

One of the more remarkable findings in the expression profile analysis was that the D and N subpopulations of asymptomatic carriers clustered within the same group as those of the indolent ATL cases (Fig. 5A and B). The asymptomatic carriers used in this analysis had high PVLs and relatively high proportions of the D and N subpopulations (Supplementary Table S1). In addition, mono- or oligoclonal expansion of the HTLV-I–infected cells was demonstrated in these cases. HTLV-I–infected cells in the D and N subpopulations of these asymptomatic carriers comprise clonally expanding cells that are potentially at the premalignant and intermediate stages according to their clonality, comprehensive gene expression profile, miR31 expression, and aberrant RNA splicing, all indicating that they can be categorized as asymptomatic carriers with high risk of developing into ATL, requiring careful follow-up (15, 30, 33, 34). Our flow-cytometric analysis of PBMCs from asymptomatic carriers using the CADM1 versus CD7 plot may provide a powerful tool for identifying high-risk asymptomatic carriers. Certain indolent ATL cases are difficult to distinguish from asymptomatic carriers, according to Shimoyama's criteria based on the morphologic characteristics determined by microscopic examination. Characterization of peripheral blood T cells by the CADM1 versus CD7 plot may provide useful information for clinical diagnosis.

According to Masuda and colleagues, manipulation of *CADM1* gene expression in leukemic cell lines suggested that CADM1 expression confers upon ATL cells tissue invasiveness and a growth advantage (35). The mechanism by which HTLV-I infection regulates CADM1 expression and the significance of CADM1 expression in ATL oncogenesis will require clarification by future studies.

Finally, as summarized in Supplementary Fig. S5, we demonstrated that (1) HTLV-I–infected and clonally expanded cells are efficiently enriched in $CADM1^+$ subpopulations; (2) the proportions of the three subpopulations in the CADM1 versus CD7 plot, discriminated by CADM1 expression and stepwise downregulation of CD7, accurately reflect the disease stage in HTLV-I infection; and (3) the $CADM1^+CD7^{dim/neg}$ subpopulations are at the intermediate stage of ATL progression and can be identified even in asymptomatic carriers. These findings will help to elucidate the molecular events involved in multistep oncogenesis of ATL.

Disclosure of Potential Conflicts of Interest

No potential conflicts of interest were disclosed.

Authors' Contributions

Conception and design: S. Kobayashi, T. Watanabe, K. Uchimaru
Development of methodology: T. Ishigaki, T. Yamochi, N. Watanabe

Published OnlineFirst April 11, 2014; DOI: 10.1158/1078-0432.CCR-13-3169

Acquisition of data (provided animals, acquired and managed patients, provided facilities, etc.): S. Kobayashi, E. Watanabe, K. Yuji, N. Oyaizu, S. Asanuma, A. Tojo
Analysis and interpretation of data (e.g., statistical analysis, biostatistics, computational analysis): S. Kobayashi, K. Nakano, T. Ishigaki, N. Oyaizu, M. Yamagishi, T. Watanabe
Writing, review, and/or revision of the manuscript: S. Kobayashi, K. Nakano, A. Tojo, T. Watanabe, K. Uchimaru
Administrative, technical, or material support (i.e., reporting or organizing data, constructing databases): T. Ishigaki, N. Ohno, N. Watanabe
Study supervision: A. Tojo, T. Watanabe, K. Uchimaru

Acknowledgments

The authors thank Drs. Kazunari Yamaguchi (National Institute of Infectious Diseases, Tokyo, Japan) and Yoshinori Murakami (the University of Tokyo) for their constructive comments; Yuji Zaike (Clinical Laboratory, Research Hospital, Institute of Medical Science, the University of Tokyo) for his excellent technical advice; Keisuke Takahashi, Sanae Suzuki, and members of our laboratory for assistance; and the hospital staff, which has made a commitment to providing high-quality care to all patients. The English in this document has been checked by at least two professional editors, both native speakers of English.

Grant Support

This work was supported by grants-in-aid for scientific research awarded to K. Uchimaru (no. 22591028) and T. Watanabe (no. 23390250) by the Ministry of Education, Culture, Sports, Science and Technology of Japan.

The costs of publication of this article were defrayed in part by the payment of page charges. This article must therefore be hereby marked *advertisement* in accordance with 18 U.S.C. Section 1734 solely to indicate this fact.

Received November 19, 2013; revised March 19, 2014; accepted March 26, 2014; published OnlineFirst April 11, 2014.

References

1. Yoshida M, Miyoshi I, Hinuma Y. Isolation and characterization of retrovirus from cell lines of human adult T-cell leukemia and its implication in the disease. Proc Natl Acad Sci U S A 1982;79:2031–5.
2. Osame M, Usuku K, Izumo S, Ijichi N, Amitani H, Igata A, et al. HTLV-I associated myelopathy, a new clinical entity. Lancet 1986;1:1031–2.
3. Mochizuki M, Watanabe T, Yamaguchi K, Takatsuki K, Yoshimura K, Shirao M, et al. HTLV-I uveitis: a distinct clinical entity caused by HTLV-I. Jpn J Cancer Res 1992;83:236–9.
4. Yamaguchi K, Watanabe T. Human T lymphotropic virus type-I and adult T-cell leukemia in Japan. Int J Hematol 2002;76 Suppl 2:240–5.
5. Murphy EL, Hanchard B, Figueroa JP, Gibbs WN, Lofters WS, Campbell M, et al. Modelling the risk of adult T-cell leukemia/lymphoma in persons infected with human T-lymphotropic virus type I. Int J Cancer 1989;43:250–3.
6. Iwanaga M, Watanabe T, Yamaguchi K. Adult T-cell leukemia: a review of epidemiological evidence. Front Microbiol 2012;3:322.
7. Okamoto T, Ohno Y, Tsugane S, Watanabe S, Shimoyama M, Tajima K, et al. Multi-step carcinogenesis model for adult T-cell leukemia. Jpn J Cancer Res 1989;80:191–5.
8. Matsuoka M, Jeang KT. Human T-cell leukemia virus type 1 (HTLV-1) and leukemic transformation: viral infectivity, Tax, HBZ and therapy. Oncogene 2011;30:1379–89.
9. Matsuoka M, Jeang KT. Human T-cell leukaemia virus type 1 (HTLV-1) infectivity and cellular transformation. Nat Rev Cancer 2007;7:270–80.
10. Yoshida M. Molecular approach to human leukemia: isolation and characterization of the first human retrovirus HTLV-1 and its impact on tumorigenesis in adult T-cell leukemia. Proc Jpn Acad Ser B Phys Biol Sci 2010;86:117–30.
11. Yamagishi M, Watanabe T. Molecular hallmarks of adult T cell leukemia. Front Microbiol 2012;3:334.
12. Tsukasaki K, Hermine O, Bazarbachi A, Ratner L, Ramos JC, Harrington W Jr, et al. Definition, prognostic factors, treatment, and response criteria of adult T-cell leukemia-lymphoma: a proposal from an international consensus meeting. J Clin Oncol 2009;27:453–9.
13. Ishida T, Joh T, Uike N, Yamamoto K, Utsunomiya A, Yoshida S, et al. Defucosylated anti-CCR4 monoclonal antibody (KW-0761) for relapsed adult T-cell leukemia-lymphoma: a multicenter phase II study. J Clin Oncol 2012;30:837–42.
14. Tian Y, Kobayashi S, Ohno N, Isobe M, Tsuda M, Zaike Y, et al. Leukemic T cells are specifically enriched in a unique CD3(dim) CD7(low) subpopulation of CD4(+) T cells in acute-type adult T-cell leukemia. Cancer Sci 2011;102:569–77.
15. Kobayashi S, Tian Y, Ohno N, Yuji K, Ishigaki T, Isobe M, et al. The CD3 versus CD7 Plot in Multicolor Flow Cytometry Reflects Progression of Disease Stage in Patients Infected with HTLV-I. PLoS One 2013;8:e53728.
16. Reinhold U, Abken H. CD4+ CD7- T cells: a separate subpopulation of memory T cells? J Clin Immunol 1997;17:265–71.
17. Reinhold U, Abken H, Kukel S, Moll M, Muller R, Oltermann I, et al. CD7- T cells represent a subset of normal human blood lymphocytes. J Immunol 1993;150:2081–9.
18. Leblond V, Othman TB, Blanc C, Theodorou I, Choquet S, Sutton L, et al. Expansion of CD4+CD7- T cells, a memory subset with preferential interleukin-4 production, after bone marrow transplantation. Transplantation 1997;64:1453–9.
19. Aandahl EM, Quigley MF, Moretto WJ, Moll M, Gonzalez VD, Sonnerborg A, et al. Expansion of CD7(low) and CD7(negative) CD8 T-cell effector subsets in HIV-1 infection: correlation with antigenic load and reversion by antiretroviral treatment. Blood 2004;104:3672–8.
20. Autran B, Legac E, Blanc C, Debre P. A Th0/Th2-like function of CD4+CD7- T helper cells from normal donors and HIV-infected patients. J Immunol 1995;154:1408–17.
21. Legac E, Autran B, Merle-Beral H, Katlama C, Debre P. CD4+CD7-CD57+ T cells: a new T-lymphocyte subset expanded during human immunodeficiency virus infection. Blood 1992;79:1746–53.
22. Schmidt D, Goronzy JJ, Weyand CM. CD4+ CD7- CD28- T cells are expanded in rheumatoid arthritis and are characterized by autoreactivity. J Clin Invest 1996;97:2027–37.
23. Willard-Gallo KE, Van de Keere F, Kettmann R. A specific defect in CD3 gamma-chain gene transcription results in loss of T-cell receptor/CD3 expression late after human immunodeficiency virus infection of a CD4+ T-cell line. Proc Natl Acad Sci U S A 1990;87:6713–7.
24. Sasaki H, Nishikata I, Shiraga T, Akamatsu E, Fukami T, Hidaka T, et al. Overexpression of a cell adhesion molecule, TSLC1, as a possible molecular marker for acute-type adult T-cell leukemia. Blood 2005;105:1204–13.
25. Nakahata S, Morishita K. CADM1/TSLC1 is a novel cell surface marker for adult T-cell leukemia/lymphoma. J Clin Exp Hematop 2012;52:17–22.
26. Kuramochi M, Fukuhara H, Nobukuni T, Kanbe T, Maruyama T, Ghosh HP, et al. TSLC1 is a tumor-suppressor gene in human non-small-cell lung cancer. Nat Genet 2001;27:427–30.
27. Nakahata S, Saito Y, Marutsuka K, Hidaka T, Maeda K, Hatakeyama K, et al. Clinical significance of CADM1/TSLC1/IgSF4 expression in adult T-cell leukemia/lymphoma. Leukemia 2012;26:1238–46.
28. Sugamura K, Fujii M, Kannagi M, Sakitani M, Takeuchi M, Hinuma Y. Cell surface phenotypes and expression of viral antigens of various human cell lines carrying human T-cell leukemia virus. Int J Cancer 1984;34:221–8.
29. Shimoyama M. Diagnostic criteria and classification of clinical subtypes of adult T-cell leukaemia-lymphoma. A report from the Lymphoma Study Group (1984–87). Br J Haematol 1991;79:428–37.
30. Iwanaga M, Watanabe T, Utsunomiya A, Okayama A, Uchimaru K, Koh KR, et al. Human T-cell leukemia virus type I (HTLV-1) proviral load and

Published OnlineFirst April 11, 2014; DOI: 10.1158/1078-0432.CCR-13-3169

disease progression in asymptomatic HTLV-1 carriers: a nationwide prospective study in Japan. Blood 2010;116:1211–9.

31. Yamagishi M, Nakano K, Miyake A, Yamochi T, Kagami Y, Tsutsumi A, et al. Polycomb-mediated loss of miR-31 activates NIK-dependent NF-kappaB pathway in adult T cell leukemia and other cancers. Cancer Cell 2012;21:121–35.
32. Asanuma S, Yamagishi M, Kawanami K, Nakano K, Sato-Otsubo A, Muto S, et al. Adult T-cell leukemia cells are characterized by abnormalities of Helios expression that promote T-cell growth. Cancer Sci 2013;104:1097–106.
33. Yamaguchi K, Kiyokawa T, Nakada K, Yul LS, Asou N, Ishii T, et al. Polyclonal integration of HTLV-I proviral DNA in lymphocytes from HTLV-I seropositive individuals: an intermediate state between the healthy carrier state and smouldering ATL. Br J Haematol 1988;68: 169–74.
34. Kamihira S, Iwanaga M, Doi Y, Sasaki D, Mori S, Tsurda K, et al. Heterogeneity in clonal nature in the smoldering subtype of adult T-cell leukemia: continuity from carrier status to smoldering ATL. Int J Hematol 2012;95:399–408.
35. Masuda M, Maruyama T, Ohta T, Ito A, Hayashi T, Tsukasaki K, et al. CADM1 interacts with Tiam1 and promotes invasive phenotype of human T-cell leukemia virus type I-transformed cells and adult T-cell leukemia cells. J Biol Chem 2010;285: 15511–22.